Journal of Solar Energy Research (JSER)

Journal homepage: www.jser.ut.ac.ir

# Solar Irradiance Variability and Its Impact On PV-Battery Standalone System Sizing and Techno-Economic Performance Across Different Climatic Regions

Anthony Chibuike Ohajianya[a,*], Ebiyibo Collins Ouserigha[b], James Abumchukwu Ezihe[a], Festus Uchenna Nwaneho[a], Benjamin Okechukwu Okereke[a], Joseph Chukwuma Echewodo[a], Chikodiri Marymartha Ugbaja[a], Mustapha Shehu[c]

[a]*Department of Physics, Federal University of Technology, Owerri, Nigeria*
[b]*Department of Physics, Niger Delta University, Amassoma, Nigeria*
[c]*Department of Physics, Federal University Dutse, Jigawa State, Nigeria*

**ARTICLE INFO**

**Article Type:**

**Research Article**

**Received:2026.05.18**
**Accepted in revised form:2026.06.19**

**Keywords**:
Solar irradiance variability; Standalone PV systems; Battery storage sizing; System reliability; Energy yield; Techno-economic analysis

**A B S T R A C T**

Solar irradiance variability significantly influences the sizing, reliability, battery ageing, and economic performance of standalone photovoltaic (PV) systems with battery storage. This study investigates these impacts across six climatically diverse locations: Abuja (Nigeria), Amman (Jordan), Paris (France), Ottawa (Canada), Santiago (Chile), and Canberra (Australia). Daily and monthly solar irradiation data from PVGIS TMY 5.3 were used to evaluate variability using the coefficient of variation (CV) and seasonal variability index (SVI). Three PV sizing approaches—daily-based, average-based, and critical-month—were assessed using a daily energy-balance model, while techno-economic performance was evaluated using PVsyst. Results show that Abuja and Amman exhibited low variability (CV < 0.50; SVI < 1.00), whereas Paris and Ottawa showed high variability (CV > 0.60; SVI > 1.40). Critical-month sizing increased PV capacity requirements by approximately 332% and 188% in Paris and Ottawa, respectively, compared with average-based sizing, but by only 39% and 89% in Abuja and Amman. Reliability improved substantially under critical-month sizing (LPSP < 0.02), although at higher lifecycle costs. Annual battery capacity fade ranged from 1.46% to 1.73%, corresponding to battery lifetimes of 12.8–15.2 years. These findings highlight the importance of incorporating irradiance variability into climate-responsive PV–battery system design.

*Corresponding Author Email:anthony.ohajianya@futo.edu.ng

**Cite this article:** Ohajianya, A. Chibuike, Ouserigha, E. Collins, Ezihe, J. Abumchukwu, Nwaneho, F. Uchenna, Okereke, B. Okechukwu, Echewodo, J. Chukwuma, Ugbaja, C. Marymartha and Shehu, M. (2026). Solar Irradiance Variability and Its Impact On PV-Battery Standalone System Sizing and Techno-Economic Performance Across Different Climatic Regions. Journal of Solar Energy Research, 11(2), 3055-3077. doi: 10.22059/jser.2026.414676.1742

DOI: 10.22059/jser.2026.414676.1742

## 1. Introduction

The global transition toward sustainable energy systems has intensified the deployment of photovoltaic (PV) technologies across diverse climatic regions [1-4]. Solar energy offers a clean, abundant, and increasingly cost-competitive alternative to conventional fossil-fuel-based electricity generation [5-7]. In many parts of the world, particularly in regions with limited grid reliability or high electricity costs, standalone PV systems integrated with battery storage have emerged as a viable solution for decentralized energy supply [8-10]. These systems are especially critical for off-grid and energy-access applications, where continuous and reliable power delivery is essential [11, 12].

The performance and design of PV systems are fundamentally governed by the availability and temporal distribution of solar irradiance [13-17]. Traditionally, PV system sizing and performance assessment rely on average annual solar irradiation metrics, such as global horizontal irradiation (GHI) [18-20]. While such metrics provide a convenient basis for preliminary system design, they often fail to capture the variability inherent in solar resource availability [21, 22]. Solar irradiance exhibits significant fluctuations on seasonal and inter-monthly scales, influenced by geographical location, atmospheric conditions, and climatic patterns [23-26]. These variations can lead to periods of reduced energy generation, which are particularly critical for standalone PV systems that depend on stored energy to maintain supply continuity [27].

In PV-battery standalone systems, irradiance variability has a compounded impact, affecting not only the energy yield of the PV array but also the required capacity of the battery storage system [28-31]. During periods of high solar availability, excess energy can be stored in the battery, while during low-irradiance periods, stored energy must be sufficient to meet the load demand [32]. Consequently, inadequate consideration of irradiance variability in system design can result in under-sized PV arrays or insufficient battery capacity, leading to energy deficits and reduced system reliability [33-35]. Conversely, overly conservative designs may lead to excessive system costs due to unnecessary oversizing of components [36].

Previous studies have examined the influence of solar resource availability on PV system performance and sizing [37-39]. It is well established that temperature effects, module characteristics, and system losses influence PV energy output [40, 41]. Additionally, several works have highlighted the importance of incorporating variability metrics, such as the coefficient of variation, in solar resource assessment [19, 21, 25, 42]. However, most existing studies focus either on single-location analyses or on PV-only systems, with limited attention given to the integrated effect of irradiance variability on both PV and battery sizing across multiple climatic regions. Furthermore, many design approaches continue to rely on average solar resource values, without explicitly accounting for seasonal fluctuations that are critical in standalone applications. For instance, the studies by Hashemian and Noorpoor [43, 44], Al-Maqsoosi et al. [45], Chiteka and Enweremadu [46], Karamshahlu et al. [47], and Faridah et al. [48], provided valuable insights into renewable energy system design and optimization. However, these investigations were conducted for single locations, thereby limiting the generalizability of their findings across regions with different climatic conditions and solar resource variability. In addition, very few studies have simultaneously examined irradiance variability, battery aging, reliability performance, and techno-economic indicators across multiple climatic regions using a common design framework.

To address the identified research gap, this study investigates the impact of solar irradiance variability on the sizing, reliability, battery aging, and techno-economic performance of standalone PV–battery systems across six climatically diverse locations: Abuja (Nigeria), Amman (Jordan), Paris (France), Ottawa (Canada), Santiago (Chile), and Canberra (Australia). Solar irradiance variability is quantified using the coefficient of variation (CV) and seasonal variability index (SVI), while system sizing is performed using daily-based, average-based, and critical-month design approaches. The resulting PV–battery configurations are subsequently evaluated through daily energy-balance analysis, battery lifetime assessment, and techno-economic evaluation to determine their technical and economic implications under different climatic conditions.

Unlike previous studies that focused primarily on single locations or considered PV sizing without explicitly examining the role of irradiance variability, this study provides a comparative assessment across multiple climatic regions and links solar variability directly to system sizing requirements, reliability performance, battery degradation, and lifecycle economics. By integrating variability metrics, reliability analysis, battery aging assessment, and techno-economic evaluation within

a common framework, the study offers a broader understanding of climate-responsive PV–battery system design and provides practical insights for the deployment of reliable and cost-effective standalone renewable-energy systems.

## 2. Methodology

### 2.1 Study locations and solar resource data

This study evaluates the impact of solar irradiance variability on photovoltaic (PV)–battery standalone system sizing across six geographically and climatically diverse locations: Abuja (Nigeria), Amman (Jordan), Paris (France), Ottawa (Canada), Santiago (Chile), and Canberra (Australia). These locations were selected to represent a wide range of climatic conditions, including tropical (Abuja), arid (Amman), temperate (Paris), continental (Ottawa), Mediterranean/subtropical (Santiago), and temperate-subtropical (Canberra) climates. This diversity enables a comprehensive assessment of how climatic variability influences solar resource availability and, consequently, PV-battery system design.

Daily solar irradiation and average ambient temperature as well as monthly average daily solar irradiation and temperature data were obtained for each location from a validated meteorological database (PVGIS TMY 5.3). The data were processed to obtain the annual irradiation, annual mean irradiation, monthly distributions, and minimum monthly irradiation values required for system design. The coordinate of the locations as well as the global horizontal irradiation (GHI) and ambient temperature are presented in Table 1.

Table 1. Study location with their GHI and average ambient temperature

| S/N | Location | Coordinates | GHI (kWh/m$^2$/yr) | $T_a$ ($^0$C) |
|---|---|---|---|---|
| 1 | Abuja | 9.0643$^0$ N, 7.4893$^0$ E | 2,042 | 26.6 |
| 2 | Amman | 31.9516$^0$ N, 35.9240$^0$ E | 2,095 | 17.9 |
| 3 | Paris | 48.8569$^0$ N, 2.3508$^0$ E | 1,190 | 11.8 |
| 4 | Ottawa | 45.4204$^0$ N, 75.6924$^0$ W | 1,312 | 6.6 |
| 5 | Santiago | 33.5739$^0$ S, 70.6206$^0$ W | 2,061 | 13.6 |
| 6 | Canberra | 35.2984$^0$ S, 149.1340$^0$ E | 1,729 | 12.6 |

### 2.2 Quantification of irradiance variability

To characterize solar resource variability across the selected locations, statistical indices were employed.

**Coefficient of Variation:** The coefficient of variation (CV) provides a normalized measure of intra-annual variability. It was calculated using equation (1) [49]:

$$CV = \frac{\sigma}{\mu} \quad (1)$$

where σ is the standard deviation of monthly average irradiation and μ is the annual mean irradiation.

**Seasonal Variability Index:** The seasonal variability index (SVI) quantifies the magnitude of seasonal fluctuations and is particularly relevant for standalone system design. It was defined for this study and computed using equation (2).

$$SVI = \frac{H_{\max} - H_{\min}}{H_{avg}} \quad (2)$$

where $H_{max}$ and $H_{min}$ are the maximum and minimum monthly average daily irradiation values while $H_{avg}$ is the annual average daily irradiation.

### 2.3 System design parameters and assumptions

To ensure consistency across all locations, fixed daily load demand and identical system configurations were adopted. The assumed system design parameters are as presented in Table 2.

Table 2. Assumed system design parameters

| S/N | Parameter | Value |
|---|---|---|
| 1 | Nominal Operating Cell Temperature, NOCT ($^0$C) | 45 |
| 2 | Solar Irradiance for Cell Tem. Comp., G (W/m$^2$) | 800 |
| 3 | Temperature Coefficient, β (/$^0$C) | 0.0036 |
| 4 | Inverter Efficiency, $\eta_{inv}$ | 0.95 |
| 5 | Wiring Efficiency, $\eta_{wire}$ | 0.98 |
| 6 | Miscellaneous system efficiency, $\eta_{other}$ | 0.93 |
| 7 | Battery Efficiency, $\eta_{batt}$ | 0.90 |
| 8 | Battery Charging Efficiency, $\eta_{ch}$ | 0.95 |
| 9 | Battery Discharging Efficiency, $\eta_{dis}$ | 0.95 |
| 10 | Daily Load Demand (kWh/d), $E_d$ (kWh/day) | 10 |
| 11 | Number of Days of Autonomy, $N_{aut}$ | 1.50 |

| | | |
|---|---|---|
| | (days) | |
| 12 | Maximum Depth of Discharge, $DoD_{max}$ | 0.80 |

### 2.4 PV system sizing

Three PV sizing approaches were adopted to evaluate the influence of irradiance variability.

#### 2.4.1 Daily-based PV sizing

The required PV capacity, $P_{PV}$ (kWp) was computed using equation (3) [50]:

$$P_{pv} = \frac{\sum_{d=1}^{365} \frac{E_d}{H_{eq,d} \times PR_d}}{365} \quad (3)$$

where $E_d$ (kWh/day) = daily load demand, which is assumed constant in this study; $H_{eq,d}$ (kWh/kWp/day) = equivalent daily peak sun hour; and $PR_d$ = daily performance ratio.

Performance ratio which represents the ratio of real PV output ($E_{actual}$) to theoretical output under standard conditions ($E_{ideal}$) was estimated from loss factors equation (4) [13]:

$$PR = \eta_{inv} \times \eta_{temp} \times \eta_{wiring} \times \eta_{other} \quad (4)$$

Where $\eta_{inv}$ = inverter efficiency, $\eta_{temp}$ = temperature-loss factor, $\eta_{wiring}$ = wiring efficiency, and $\eta_{other}$ = miscellaneous system efficiency.

The temperature-loss factor, $\eta_{temp}$, was computed using equation (5) while the required cell temperature, $T_c$ was calculated using equation (6) [13]:

$$\eta_{temp} = 1 - \beta\left(T_c - 25\right) \quad (5)$$

$$T_c = T_a + \frac{NOCT - 20}{800} \times G \quad (6)$$

where β is the temperature coefficient ($°C^{-1}$) representing the rate of efficiency reduction with increasing cell temperature, $T_a$ is ambient temperature, NOCT is the nominal operating cell temperature representing the typical temperature reached by PV modules under standard outdoor conditions, and G is the incident solar irradiance.

With the assumed values of β (= $0.0036/^0C$), NOCT (= $45^0C$), and G (= 800 $Wm^{-2}$), equation (5) reduces to equation (7):

$$\eta_{temp} = 1 - 0.0036T_a \quad (7)$$

Putting equation (7) into equation (4), enabled the computation of the daily performance ratio required in the PV capacity estimation equation (3).

#### 2.4.2 Average-based PV sizing

For the average-based PV sizing method, the PV capacity required for each location was calculated using equation (8) [50]:

$$P_{PV,avg} = \frac{E_d}{H_{avg} \cdot PR_{avg}} \quad (8)$$

where $E_d$ is the daily load demand (= 10 kWh/day), $H_{avg}$ is the annual average daily equivalent peak sun hours, and $PR_{avg}$ is the average performance ratio.

#### 2.4.3 Critical-month PV sizing

Here, the required PV capacity was calculated using equation (9) [50]:

$$P_{PV,crit} = \frac{E_d}{H_{\min} \cdot PR_{cm}} \quad (9)$$

Where $E_d$ is the daily load demand (= 10 kWh/day), $H_{min}$ is the minimum monthly average daily irradiation equivalent peak sun hours, and $PR_{cm}$ is the average performance ratio for the critical month (the month with lowest solar irradiation).

This approach ensures system adequacy during the worst solar conditions and is essential for standalone systems.

#### 2.4.4 PV oversizing ratio

The PV oversizing ratio and required oversizing percentage which shows the impact of solar irradiance variability on PV system design was defined for this study and calculated using equation set (10):

$$\begin{cases} PV\ Oversizing\ Ratio = \dfrac{P_{PV,crit}}{P_{PV,avg}} \\ \%\ \text{Increase} = \left(\dfrac{P_{PV,critical} - P_{PV,average}}{P_{PV,average}}\right) \times 100 \end{cases} \quad (10)$$

where $P_{PV,crit}$ and $P_{PV,avg}$ are the required PV capacity calculated from the critical-month and average-based design methods, respectively.

### 2.5 Battery storage sizing

To enhance system reliability, battery storage was incorporated into the system design using an autonomy-based sizing approach.

The required battery storage capacity, $C_{bat}$(kWh) was estimated using equation (11) [51]:

$$C_{bat} = \frac{E_d \cdot N_{aut}}{\eta_{bat} \cdot DoD_{max}} \quad (11)$$

Where $N_{aut}$ is the number of autonomy days, $\eta_{bat}$ is battery efficiency, and $DoD_{max}$ is the maximum allowable depth of discharge.

### 2.6 PV-battery performance modelling and simulation using daily irradiation data

To account for storage behavior in the standalone PV system, a daily energy-balance battery model was adopted using 365 daily irradiation values for each study location. For each day d, the PV energy generated was estimated from the installed PV capacity, daily solar irradiation, and location-specific performance ratio using equation (12) [51]:

$$E_{PV,d} = P_{PV}\, H_d\, PR \quad (12)$$

where $E_{PV,d}$ is the PV energy generated on day d (kWh/day), $P_{PV}$ is the installed PV capacity (kW), $H_d$ is the daily solar irradiation or equivalent peak sun hours on day d, and PR is the performance ratio.

The daily net energy balance was obtained using equation (13) [51]:

$$\Delta E_d = E_{PV,d} - E_d \quad (13)$$

where $E_d$ is the daily load demand. A positive $\Delta E_d$ indicates surplus energy available for charging the battery, while a negative value indicates a deficit that must be supplied by the battery.

The battery state of charge was updated sequentially on a daily basis. For charging conditions ($\Delta E_d > 0$), the battery state of charge was calculated using equation (14) [51]:

$$SOC_d = \min\left[SOC_{d-1} + \eta_{ch}\Delta E_d, SOC_{\max}\right] \quad (14)$$

While for discharging conditions ($\Delta E_d < 0$), the battery state of charge was evaluated using equation (15) [51]:

$$SOC_d = \max\left[SOC_{d-1} - \frac{|\Delta E_d|}{\eta_{dis}}, SOC_{\min}\right] \quad (15)$$

where $SOC_d$ and $SOC_{d-1}$ are the battery energy content at the end of day d and day (d-1), $\eta_{ch}$ and $\eta_{dis}$ are the charging and discharging efficiencies, and $SOS_{min}$ and $SOC_{max}$ are the minimum and maximum allowable battery energy levels, respectively.

The battery operating limits were defined from the nominal battery capacity $C_{bat}$ and the maximum allowable depth of discharge $DoD_{max}$ as given in equation (16) [51]:

$$\begin{cases} SOC_{\max} = C_{bat} \\ SOC_{\min} = \left(1 - DoD_{\max}\right) C_{bat} \end{cases} \quad (16)$$

If the available PV generation and the usable battery energy were insufficient to satisfy the daily load, the remaining energy deficit was recorded as unmet load [52],

$$E_{def,d} = \max\left[0, E_{load,d} - E_{PV,d} - \eta_{dis}\left(SOC_{d-1} - SOC_{\min}\right)\right] \quad (17)$$

The annual system reliability was assessed using the loss of power supply probability (LPSP) [53],

$$LPSP = \frac{\sum_{d=1}^{365} E_{def,d}}{\sum_{d=1}^{365} E_d} \quad (18)$$

and the corresponding reliability index,

$$R = 1 - LPSP \quad (19)$$

This daily modelling approach captures day-to-day fluctuations in solar resource availability and provides a more realistic assessment of PV-battery standalone system adequacy than monthly average design alone, while remaining simpler than full hourly simulation.

The surplus energy that could not be stored due to battery capacity limitations was calculated for each day using equation (20) [54]. When the battery reached its maximum state of charge, any additional PV energy exceeding the combined load demand and available storage capacity was treated as wasted energy. This was quantified by comparing the daily surplus energy with the available storage space, accounting for charging efficiency.

$$E_{waste,d} = \max\left[0, \Delta E_d - \frac{SOC_{\max} - SOC_{d-1}}{\eta_{ch}}\right] \quad (20)$$

**Total annual wasted energy,**

$$E_{waste,annual} = \sum_{d=1}^{365} E_{waste,d} \quad (21)$$

**Fraction of wasted energy,**

$$\text{Wasted energy fraction} = \frac{E_{waste,annual}}{\sum_{d=1}^{365} E_{PV,d}} \quad (22)$$

An excel-based design and simulation template was developed by coding the appropriate equations into the excel cells and making provisions for pasting the design assumptions and meteorological data. With this, the PV-battery system was designed and simulated for the six study locations.

### 2.7 Battery capacity fade and lifetime modelling

Battery degradation influences the long-term performance, reliability, and economic viability of standalone PV–battery systems. To account for the effect of storage aging, battery lifetime was evaluated using the battery aging and replacement framework implemented in PVsyst. Lithium Iron Phosphate (LFP) batteries were selected due to their widespread application in standalone photovoltaic systems, high cycle life, and thermal stability.

Battery aging was assumed to occur through a combination of calendar aging and cycling-related degradation. Calendar aging represents the gradual loss of battery capacity with time and is strongly influenced by operating temperature, while cycling degradation results from repeated charge-discharge processes. In PVsyst, battery lifetime is estimated based on operating conditions, battery utilization, and aging characteristics until the battery reaches its end-of-life criterion.

The battery end-of-life (EOL) condition was defined as the point at which the available battery capacity decreases to 80% of its initial rated capacity [55]. Thus,

$$C_{EOL} = 0.8C_0 \quad (23)$$

Where $C_{EOL}$ is the battery capacity at end-of-life and $C_0$ is the initial battery capacity.

The battery lifetime, L (years), was obtained directly from PVsyst simulations for each location and sizing method. To quantify the corresponding annual capacity degradation, an equivalent annual capacity fade rate was calculated assuming exponential capacity decay throughout the battery lifetime. The annual capacity fade (AF) was determined using equation (24) [56]:

$$AF = \left(1 - 0.8^{1/L}\right) \times 100 \quad (24)$$

where AF is the annual capacity fade (%/year) and L is the battery lifetime (years).

The remaining battery capacity after (t) years of operation was estimated using equation (25) [57]:

$$C_t = C_0(1 - AF_d)^t \quad (25)$$

where $C_t$ is the remaining battery capacity after t years and $AF_d$ is the annual capacity fade expressed as a decimal fraction.

To assess the influence of climatic conditions on battery aging, average ambient temperature was considered as an indicator of thermal stress. Locations with higher operating temperatures are expected to experience faster degradation and shorter battery lifetimes than cooler locations. Consequently, the estimated battery lifetime and annual capacity fade were compared across all study locations to evaluate the combined effects of climatic conditions and PV sizing strategies on long-term storage performance.

The resulting battery lifetime and capacity fade metrics were subsequently incorporated into the techno-economic assessment through replacement scheduling and lifecycle cost calculations.

### 2.8 Economic evaluation

A techno-economic assessment was performed to compare the economic implications of the daily-based, average-based, and critical-month PV–battery sizing approaches across the six study locations. The evaluation considered component procurement costs, project operating expenses, battery replacement requirements, photovoltaic module degradation, and discounted lifecycle costs. The principal economic indicators used in this study were the capital expenditure (CAPEX), annual operating expenditure (OPEX), net present cost (NPC), and levelized cost of energy (LCOE).

To estimate the hardware procurement costs of the PV–battery standalone systems, free-on-board (FOB) component prices were obtained from recent global benchmark reports. Monocrystalline silicon PV modules were priced at USD 0.12/Wp based on the IEA-PVPS Global Trends Report [58], lithium iron phosphate (LFP) battery packs at USD 81/kWh according to the BloombergNEF Energy Storage Market Survey [59], and hybrid inverters at USD

160/kW following the NREL Annual Technology Baseline cost benchmarks [60].

Since FOB prices represent factory-gate costs and do not reflect regional procurement conditions, location-specific cost multipliers were applied to obtain localized component costs for each study location. These multipliers were developed using regional cost information derived from IRENA total installed cost statistics, national renewable energy market reports, and published cost benchmark studies [58, 61]. The multipliers account for differences in transportation, import duties, taxes, distribution margins, labour costs, and other market-specific factors affecting equipment procurement and deployment. Lower multipliers were applied to locations with relatively mature renewable-energy supply chains and favourable import conditions, such as Santiago, while moderately higher multipliers were adopted for developed markets such as Paris and Canberra to reflect higher labour and installation costs. The highest multiplier was assigned to Abuja to account for the combined effects of logistics, importation, financing, and market-access constraints commonly reported in Sub-Saharan African renewable-energy projects. The resulting localized component costs provide a more realistic basis for the techno-economic assessment while preserving the comparative analysis of PV–battery system sizing across different climatic regions.

The localized component cost was determined as

$$C_{local} = M_{loc} \times C_{FOB} \quad (26)$$

where $C_{local}$ is the localized component cost, $M_{loc}$ is the location-specific cost multiplier, and $C_{FOB}$ is the global benchmark free-on-board cost.

The total capital expenditure (CAPEX) of each PV–battery system was computed as

$$CAPEX = C_{PV} + C_{bat} + C_{inv} + C_{other} \quad (27)$$

where $C_{PV}$, $C_{bat}$, $C_{inv}$, and $C_{other}$ represent the costs of the photovoltaic array, battery bank, hybrid inverter, and other components including installation and logistics, respectively. Based on established standalone residential PV system cost analyses in the literature [62], $C_{BOS}$ was assumed in this study to be 50% of $C_{PV}$.

The yearly operating expenditure (OPEX) comprises repair and maintenance (R&M) costs and a yearly provision for battery replacement. The repair and maintenance component of OPEX was assumed to be 1.5% of CAPEX. This assumption is consistent with the reported values for residential PV systems [62, 63].

Discount rates were selected to reflect country-specific financing conditions, investment risks, inflation expectations, and the cost of capital associated with renewable-energy projects in each study location. The adopted values were derived from published renewable-energy economic assessments, national energy investment reports, and international financing benchmarks [64-66]. Higher discount rates were assigned to developing economies with greater perceived investment and financing risks, such as Nigeria (12%) and Jordan (8%), whereas lower rates were adopted for mature and relatively stable markets, including France and Canada (5%). Intermediate values were applied to Chile (7%) and Australia (6%) to reflect their respective financing environments. These discount rates were subsequently used in the calculation of present-value economic indicators, including lifecycle cost and levelized cost of energy (LCOE), thereby enabling a more realistic comparison of the long-term economic performance of PV–battery standalone systems across different climatic and economic regions.

The capital recovery factor (CRF), used to annualize capital investments, was calculated using equation (28) [67]:

$$CRF = \frac{i(1+i)^n}{(1+i)^n - 1} \quad (28)$$

where i is the discount rate and n is the project lifetime (years). The project lifetime was assumed to be 25 years.

Photovoltaic module degradation was incorporated into the techno-economic analysis to account for the gradual reduction in energy output over the project lifetime. Annual degradation rates were assigned on a location-specific basis to reflect the influence of climatic conditions, particularly temperature, humidity, ultraviolet exposure, and environmental stressors that affect long-term module performance. Higher degradation rates were assumed for warmer locations such as Abuja (0.65%/yr) and Amman (0.55%/yr), where elevated operating temperatures can accelerate material aging and performance losses. Lower degradation rates were adopted for cooler climates such as Paris (0.35%/yr), Ottawa (0.40%/yr), Santiago (0.38%/yr), and Canberra (0.42%/yr), reflecting comparatively lower thermal stress. The annual degradation rates were used within the PVsyst simulations to model the progressive decline in PV energy production

throughout the project lifetime. Incorporating location-specific degradation rates enables a more realistic assessment of lifetime energy generation, net present cost, and levelized cost of energy across the different climatic regions considered in this study. The adopted degradation rates were selected from the reported ranges in the literature for monocrystalline silicon PV modules operating under comparable climatic conditions and were implemented as constant annual degradation rates throughout the project lifetime.

The annual energy production in year t was estimated in PVsyst using equation (29) [68]:

$$E_t = E_0(1-D_{PV})^t \quad (29)$$

where $E_t$ is the annual PV energy production in year t, $E_0$ is the initial annual energy production, and $D_{PV}$ is the annual PV module degradation rate.

The net present cost (NPC) was determined by discounting all capital, replacement, and operating expenditures over the project lifetime according to equation (30) [69]:

$$NPC = \sum_{t=0}^{n} \frac{C_{cost,t}}{(1+i)^t} \quad (30)$$

where $C_{cost,t}$ is the total expenditure incurred in year t, i is the discount rate, and n is the project lifetime.

The levelized cost of energy (LCOE) was obtained from the PVsyst economic module and is expressed as equation (31) [69]:

$$LCOE = \frac{\sum_{t=0}^{n} \frac{C_{cost,t}}{(1+i)^t}}{\sum_{t=1}^{n} \frac{E_t}{(1+i)^t}} \quad (31)$$

where $E_t$ is the electrical energy supplied in year t. The LCOE therefore represents the discounted cost of producing one kilowatt-hour of useful electrical energy over the entire project lifetime.

Table 3 presents the location-specific component cost assumptions, discount rates, and PV module degradation rates used for the techno-economic assessment while Figure 1 shows a representative hourly load profile of the assumed 10 kWh daily load demand for this study.

Table 3. Location-specific component cost assumptions, discount rates, and PV module degradation rates

| Location | PV Module ($/Wp) | LFP Battery ($/kWh) | Hybrid Inverter ($/kW) | i (%) | $D_{PV}$ (%/yr) |
|---|---|---|---|---|---|
| Global Benchmark (FOB) | 0.12 | 81 | 160 | - | - |
| Abuja, Nigeria | 0.22 | 135 | 245 | 12 | 0.65 |
| Amman, Jordan | 0.19 | 118 | 215 | 8 | 0.55 |
| Paris, France | 0.16 | 105 | 195 | 5 | 0.35 |
| Ottawa, Canada | 0.18 | 114 | 210 | 5 | 0.40 |
| Santiago, Chile | 0.15 | 98 | 185 | 7 | 0.38 |
| Canberra, Australia | 0.16 | 102 | 190 | 6 | 0.42 |

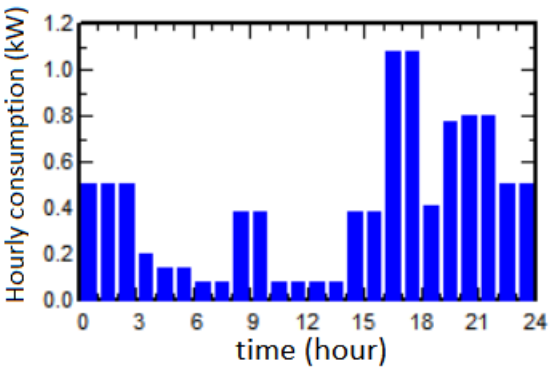


Figure 1. Assumed hourly load profile for the 10 kWh/day demand

## 3. Results and Discussion

### 3.1 Spatial distribution and solar resource characteristics

Figure 2 presents the global distribution of the selected study locations, spanning tropical, arid, temperate, continental, and subtropical climatic zones. This wide geographical spread ensures that the results capture diverse solar resource patterns and their implications for PV–battery system design.

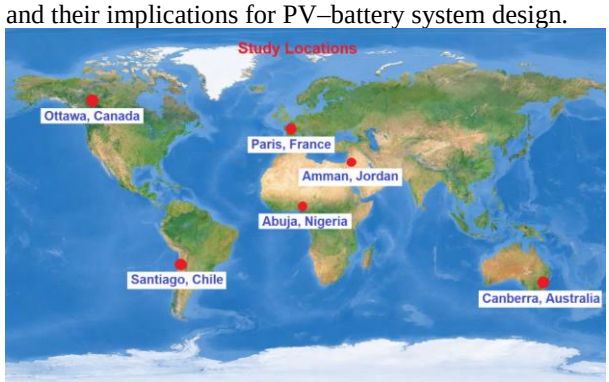


Figure 2. Global map showing study locations

The solar resource comparison in Figures 3(a) and 3(b) show clear differences in average global horizontal irradiation (GHI) across the locations. High solar resource regions such as Abuja, Amman, and Santiago exhibit average daily irradiation values above 5.5 kWh/m²/day, indicating strong solar potential. In contrast, Paris and Ottawa show significantly lower values (≈3.25–3.59 kWh/m²/day), reflecting reduced solar availability typical of higher latitudes. Canberra occupies an intermediate position.

These differences directly influence PV system sizing, as higher irradiation reduces the required PV capacity for a given load, while lower irradiation necessitates larger system sizes. However, average values alone do not fully capture system design requirements, as variability plays a critical role in standalone systems.

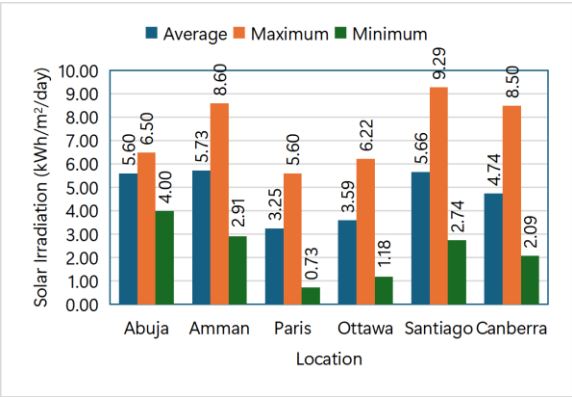


Figure 3(a). Solar resource comparison: daily average, maximum, and minimum irradiation

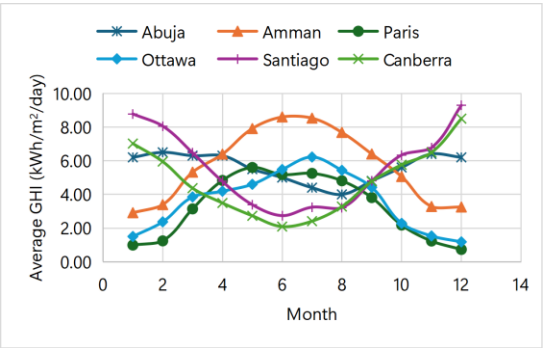


Figure 3(b). Solar resource comparison: average daily global horizontal irradiation per month

### 3.2 Irradiance variability analysis

Figure 4 presents the coefficient of variation (CV) and seasonal variability index (SVI) across the study locations. The results indicate that locations such as Paris, Ottawa and Canberra exhibit high variability, characterized by large seasonal swings between summer and winter irradiation. Conversely, Abuja and Amman show relatively low variability, with more stable year-round solar availability. Santiago exhibits intermediate variability.

High variability implies prolonged low-irradiance periods, which are critical for standalone PV systems relying on battery storage. In such locations, system design must account for worst-case conditions rather than average performance. The SVI results reinforce this observation, highlighting that continental and temperate climates experience more pronounced seasonal deficits, thereby increasing system design complexity [70-72].

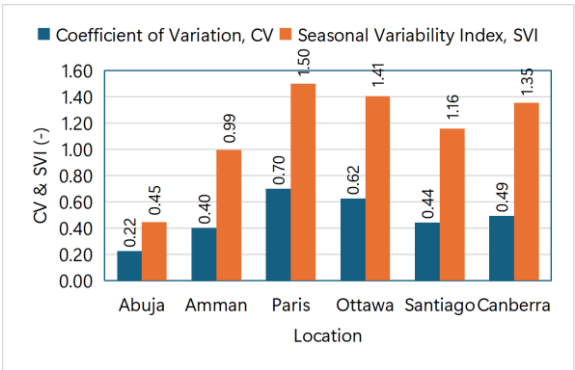


Figure 4. Variability indices across global locations

### 3.3. PV capacity requirements under different design approaches

Figure 5 compares PV capacity requirements obtained using the three sizing approaches: daily-based, average-based, and critical-month methods.

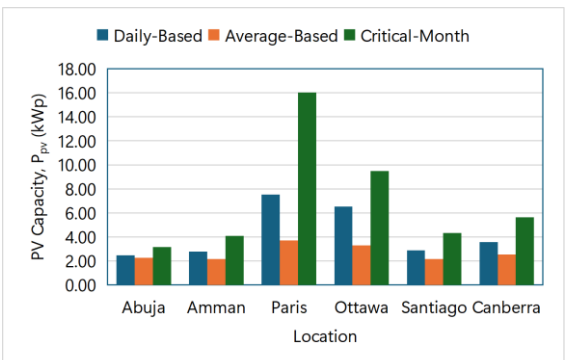


Figure 5. PV Capacity by Design Method across the locations

The results show that:

- The **average-based method** consistently yields the lowest PV capacity, as it assumes uniform solar availability throughout the year.
- The **daily-based method** produces slightly higher capacities than the average-based method in Abuja, Amman, and Santiago, and significantly higher capacities in Paris and Ottawa by accounting for day-to-day variability.
- The **critical-month method** results in the highest PV capacity, particularly in high-variability locations such as Ottawa and Paris.

This trend highlights the limitation of average-based sizing, which can significantly underestimate system requirements in regions with strong seasonal variation [33, 73]. The critical-month approach ensures energy adequacy during the worst solar conditions but may lead to overdesign in low-variability regions [74].

### 3.4 PV oversizing requirement

The PV oversizing ratio and required oversizing percentage shown in Figures 6 and 7 quantify the additional capacity required when designing for critical conditions instead of average conditions.

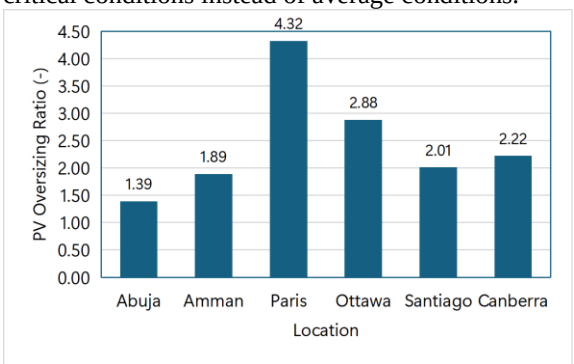


Figure 6. PV oversizing ratio across global locations

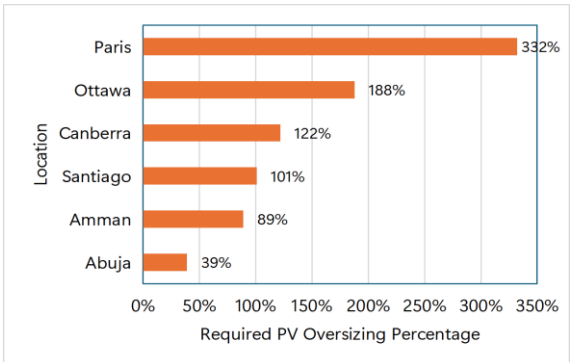


Figure 7. Required PV oversizing percentage due to irradiance variability

Locations with high variability (e.g., Ottawa and Paris) exhibit significantly higher oversizing ratios and required oversizing percentage, indicating that a large increase in PV capacity is necessary to maintain reliability.

In contrast, low-variability regions such as Abuja and Amman show relatively small oversizing requirements. This suggests that average-based design may be reasonably adequate in such climates, whereas critical-month design becomes essential in high-latitude regions.

### 3.5 Annual PV energy generation

Figure 8 shows the annual PV energy generation across the locations. As expected, locations with higher solar resource (Abuja, Amman, Santiago) generate more energy annually compared to lower-resource regions (Paris and Ottawa).

However, it is important to note that higher energy generation does not automatically translate to better system performance in standalone systems. The temporal distribution of energy is equally important, as surplus energy during high-irradiance periods may not compensate for deficits during low-irradiance periods [75, 76].

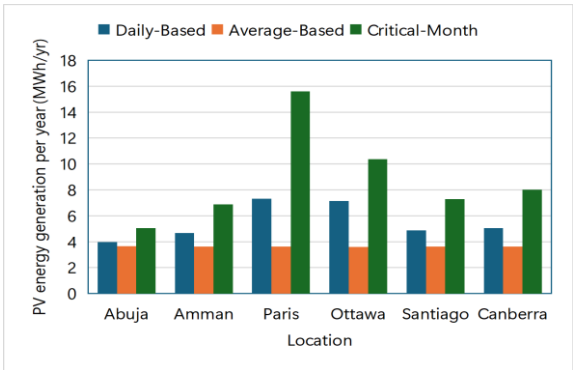


Figure 8. PV energy generation per year

### 3.6 Energy utilization and wastage

Figure 9 presents the fraction of wasted PV energy. Higher wasted energy fractions for all the design methods are observed in locations with large PV capacities and seasonal solar resource variability like Paris and Ottawa. This occurs because excess energy generated during peak periods exceeds both load demand and battery storage capacity.

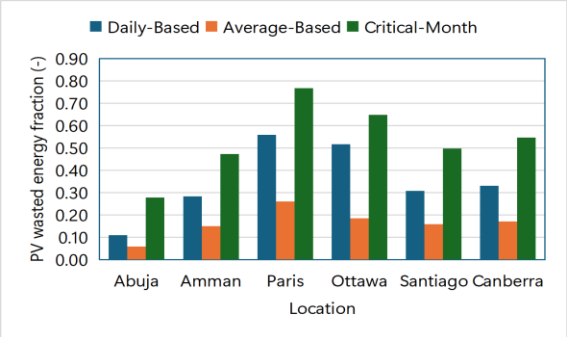


Figure 9. PV wasted energy fraction

In high-resource or low-variability regions, wasted energy is generally lower because the required PV capacity is lower and most of the generated energy is utilized to meet load demand or recharge the battery.

The results highlight a key trade-off: designing for reliability (via oversizing) often leads to increased energy wastage and reduced system efficiency.

### 3.7 System reliability and unmet load

Figures 10 and 11 show the annual unmet load and the number of unmet load days, respectively.

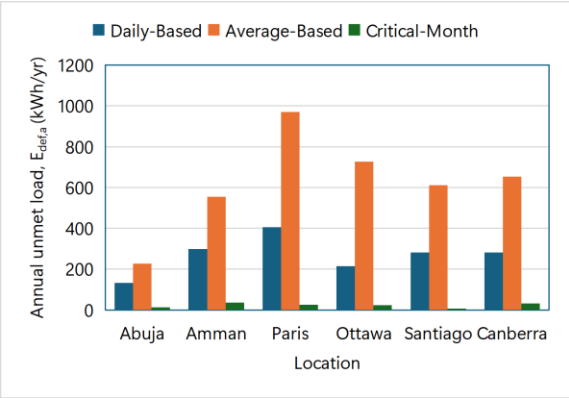


Figure 10. Annual unmet load across global locations

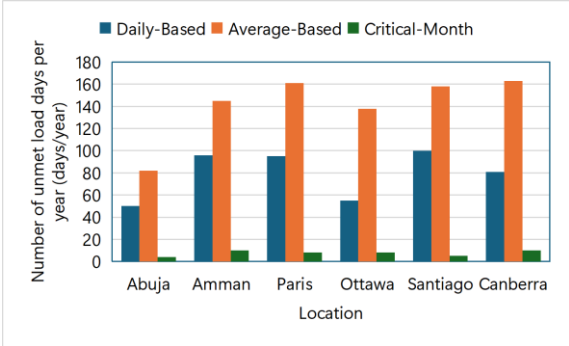


Figure 11. Number of unmet load days per year

High-variability locations exhibit significantly higher unmet load when systems are not adequately sized. This is particularly evident for designs based on average irradiation, which fail to meet demand during prolonged low-solar periods.

In contrast, locations with stable solar resources (e.g., Abuja and Amman) demonstrate minimal unmet load, indicating that system reliability is easier to achieve in such climates [77, 78].

### 3.8 Loss of power supply probability (LPSP) and reliability index

Figure 12 presents the loss of power supply probability (LPSP), while Figure 13 shows the corresponding reliability index.

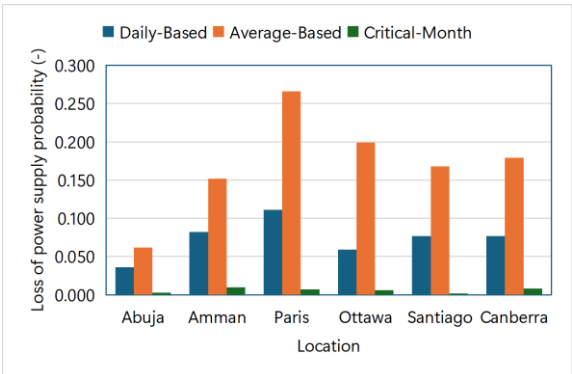


Figure 12. Loss of power supply probability, LPSP

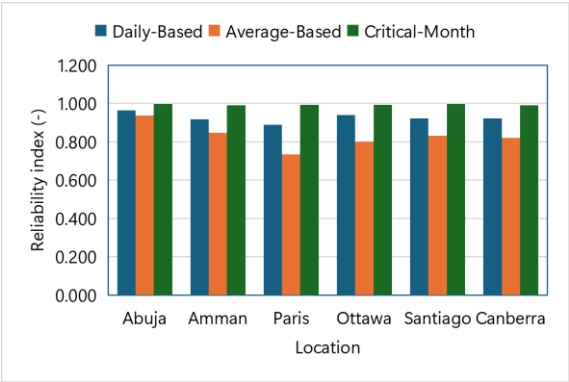


Figure 13. Reliability index across global locations

The results confirm that:

- High LPSP values are associated with high-variability regions when insufficient PV capacity or storage is provided.
- Low LPSP (and high reliability index) is achieved in locations with stable solar resources or when systems are designed using the critical-month approach.

The reliability index approaches unity in well-sized systems, particularly in tropical and arid climates. However, achieving similar reliability in temperate and continental climates requires significant system oversizing and/or increased battery capacity [33, 79].

### 3.9 Battery annual capacity fade and lifetime

Table 4 presents the estimated annual capacity fade and corresponding lifetime of the lithium iron phosphate (LFP) battery system for the six study locations. The results reveal a clear dependence of battery aging on climatic conditions, particularly ambient temperature, while showing negligible variation among the three PV sizing approaches within the same location. This indicates that temperature-induced degradation is the dominant factor influencing long-term battery performance under the assumed operating conditions.

Table 4. LFP battery annual capacity fade and lifetime

| Location | PV Sizing Method | Avg. Temp (°C) | Annual Capacity Fade (%) | Lifetime (yr) |
|---|---|---|---|---|
| Abuja | Daily-Based | 26.6 | 1.73% | 12.8 |
| | Average-Based | 26.6 | 1.73% | 12.8 |
| | Critical Month | 26.6 | 1.73% | 12.8 |
| Amman | Daily-Based | 17.9 | 1.58% | 14.0 |
| | Average-Based | 17.9 | 1.58% | 14.0 |
| | Critical Month | 17.9 | 1.58% | 14.0 |
| Paris | Daily-Based | 11.8 | 1.46% | 15.2 |
| | Average-Based | 11.8 | 1.46% | 15.2 |
| | Critical Month | 11.8 | 1.46% | 15.2 |
| Ottawa | Daily-Based | 6.6 | 1.46% | 15.2 |
| | Average-Based | 6.6 | 1.46% | 15.2 |
| | Critical Month | 6.6 | 1.46% | 15.2 |
| Santiago | Daily-Based | 13.6 | 1.46% | 15.2 |
| | Average-Based | 13.6 | 1.46% | 15.2 |
| | Critical Month | 13.6 | 1.46% | 15.2 |
| Canberra | Daily-Based | 12.6 | 1.47% | 15.1 |
| | Average-Based | 12.6 | 1.47% | 15.1 |
| | Critical Month | 12.6 | 1.47% | 15.1 |

Among the investigated locations, Abuja exhibits the highest annual capacity fade of 1.73%/yr and the shortest battery lifetime of 12.8 years. This result is attributed to its relatively high average ambient temperature of 26.6 °C, which accelerates electrochemical aging processes and increases the rate of capacity loss. Similarly, Amman, with an average temperature of 17.9 °C, records an annual capacity fade of 1.58%/yr and a battery lifetime of 14.0 years.

In contrast, the cooler locations—Paris, Ottawa, and Santiago—exhibit lower annual capacity fade rates of approximately 1.46%/yr and correspondingly longer battery lifetimes of 15.2 years. Canberra shows a slightly higher degradation rate of 1.47%/yr, resulting in a battery lifetime of 15.1 years. These findings are consistent with established battery-aging theory, which indicates that lower operating temperatures generally reduce degradation rates and extend useful battery life [80].

The results further show that the daily-based, average-based, and critical-month sizing approaches produce virtually identical battery lifetimes within each location. This suggests that differences in PV sizing have a relatively minor influence on battery aging compared with the influence of ambient climatic conditions. Consequently, while irradiance variability significantly affects PV capacity requirements, reliability, and energy utilization, battery longevity in the studied systems is governed primarily by the thermal environment.

From a practical perspective, the shorter battery lifetime observed in warmer climates implies more frequent battery replacement over the project lifetime, thereby increasing lifecycle costs.

Conversely, cooler climates benefit from reduced degradation rates and longer replacement intervals. These results highlight the importance of incorporating battery aging considerations into the techno-economic evaluation of standalone PV–battery systems, particularly when comparing system performance across different climatic regions.

The annual capacity fade decreases from 1.73%/yr in Abuja to approximately 1.46%/yr in Paris, Ottawa, and Santiago, resulting in an increase in battery lifetime from 12.8 years to about 15.2 years. This represents an approximately 19% increase in service life between the warmest and coolest study locations.

### 3.10 Economic Performance

The economic performance of the PV–battery standalone systems was evaluated using the capital expenditure (CAPEX), annual operating expenditure (OPEX), net present cost (NPC), and levelized cost of energy (LCOE). The results are presented in Tables 5 and 6 and Figures 14–16. Overall, the economic indicators closely reflect the influence of solar resource availability and irradiance variability on system sizing requirements. Locations requiring larger PV capacities generally exhibit higher investment and lifecycle costs, particularly when the critical-month sizing approach is adopted.

Table 5. Estimated CAPEX for the PV systems

| Location | PV Sizing Method | PV Module Cost ($) | LFP Battery Cost ($) | Hybrid Inverter Cost ($) | Other Costs ($) | CAPEX ($) |
|---|---|---|---|---|---|---|
| Abuja | Daily-Based | 546 | 2812 | 858 | 273 | 4489 |
| | Average-Based | 502 | 2812 | 858 | 251 | 4423 |
| | Critical Month | 695 | 2812 | 858 | 348 | 4713 |
| Amman | Daily-Based | 526 | 2458 | 753 | 263 | 4000 |
| | Average-Based | 410 | 2458 | 753 | 205 | 3826 |
| | Critical Month | 777 | 2458 | 753 | 389 | 4377 |
| Paris | Daily-Based | 1203 | 2187 | 683 | 602 | 4675 |
| | Average-Based | 594 | 2187 | 683 | 297 | 3761 |
| | Critical Month | 2562 | 2187 | 683 | 1281 | 6713 |
| Ottawa | Daily-Based | 1260 | 2375 | 735 | 630 | 5000 |
| | Average-Based | 594 | 2375 | 735 | 297 | 4001 |
| | Critical Month | 1708 | 2375 | 735 | 854 | 5672 |
| Santiago | Daily-Based | 435 | 2041 | 648 | 218 | 3342 |
| | Average-Based | 323 | 2041 | 648 | 162 | 3174 |
| | Critical Month | 648 | 2041 | 648 | 324 | 3661 |
| Canberra | Daily-Based | 570 | 2125 | 665 | 285 | 3645 |
| | Average-Based | 408 | 2125 | 665 | 204 | 3402 |
| | Critical Month | 904 | 2125 | 665 | 452 | 4146 |

Table 6. Estimated OPEX for the PV systems

| **Location** | **PV Sizing Method** | **Provision for Battery Replacement ($)** | **Repairs and Maintenance Cost ($)** | **OPEX ($)** |
|---|---|---|---|---|
| Abuja | Daily-Based | 112.48 | 67.34 | 179.82 |
| | Average-Based | 112.48 | 66.35 | 178.83 |
| | Critical Month | 112.48 | 70.69 | 183.17 |
| Amman | Daily-Based | 98.32 | 60.00 | 158.32 |
| | Average-Based | 98.32 | 57.39 | 155.71 |
| | Critical Month | 98.32 | 65.65 | 163.97 |
| Paris | Daily-Based | 87.48 | 70.12 | 157.60 |
| | Average-Based | 87.48 | 56.42 | 143.90 |
| | Critical Month | 87.48 | 100.70 | 188.18 |
| Ottawa | Daily-Based | 95.00 | 75.00 | 170.00 |

| | | | | |
|---|---|---|---|---|
| | Average-Based | 95.00 | 60.02 | 155.02 |
| | Critical Month | 95.00 | 85.08 | 180.08 |
| | Daily-Based | 81.64 | 50.12 | 131.76 |
| Santiago | Average-Based | 81.64 | 47.60 | 129.24 |
| | Critical Month | 81.64 | 54.92 | 136.56 |
| | Daily-Based | 85.00 | 54.68 | 139.68 |
| Canberra | Average-Based | 85.00 | 51.03 | 136.03 |
| | Critical Month | 85.00 | 62.19 | 147.19 |

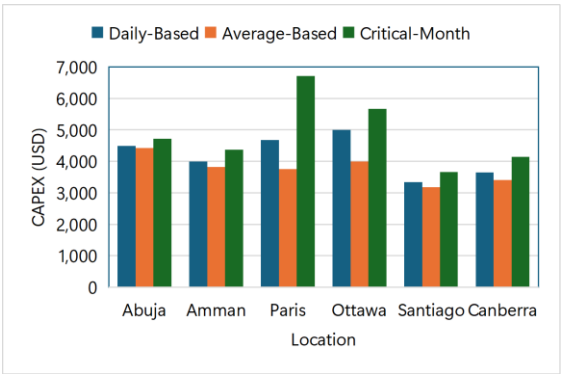


Figure 14. CAPEX comparison across design methods and global locations

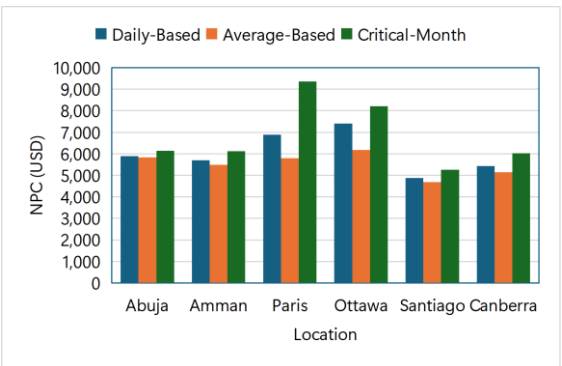


Figure 15. NPC comparison across design methods and global locations

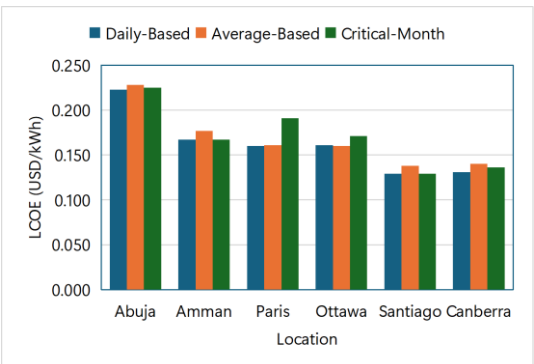


Figure 16. LCOE comparison across design methods and global locations

Figure 14 and Table 5 show the estimated CAPEX for the three sizing methods across the six study locations. For all locations, the average-based sizing method resulted in the lowest capital cost because it produced the smallest PV capacities. Conversely, the critical-month method consistently yielded the highest CAPEX due to the additional PV capacity required to satisfy energy demand during low-irradiance periods. This effect is particularly pronounced in high-variability locations such as Paris and Ottawa, where the critical-month design increased CAPEX from $3,761 to $6,713 and from $4,001 to $5,672, respectively. In contrast, lower increases were observed in low-variability locations such as Abuja and Amman, where the critical-month design raised CAPEX by less than 25% relative to the average-based approach. These findings demonstrate that climatic variability significantly influences investment requirements through its impact on PV system sizing.

The observed increase in capital cost with more conservative sizing approaches is consistent with previous studies on standalone PV systems. Researchers have reported that designs based on critical solar resource conditions generally require substantial PV oversizing to maintain energy adequacy during low-irradiance periods, leading to higher investment costs than average-resource designs. Similar trends were reported by Belmahdi et al. [81], who found that reliability-oriented sizing strategies significantly increased system capital requirements in regions with pronounced seasonal solar variability. Likewise, Lee and Callaway [82] observed that system costs rise rapidly as reliability constraints become more stringent in off-grid PV–battery applications.

The annual operating expenditure (OPEX) values presented in Table 6 exhibit trends similar to those observed for CAPEX. Since the battery replacement provision depends primarily on battery capacity and lifetime, its value remains constant across the three sizing methods within each location. Variations in OPEX therefore arise mainly from differences in repair and maintenance costs, which were assumed

to be proportional to capital investment. Consequently, systems designed using the critical-month method generally exhibit the highest OPEX, while average-based designs record the lowest values. The highest annual OPEX of $188.18 was obtained for the critical-month design in Paris, whereas the lowest value of $129.24 was recorded for the average-based design in Santiago.

The net present cost (NPC) results shown in Figure 15 indicate that lifecycle costs are strongly affected by both climatic conditions and sizing methodology. Across all locations, the average-based design produced the lowest NPC, while the critical-month design yielded the highest values due to increased initial investment and maintenance costs. The effect is particularly significant in Paris and Ottawa, where strong seasonal variability necessitates substantial PV oversizing. In Paris, the NPC increased from $5,790 for the average-based design to $9,366 for the critical-month design, representing an increase of approximately 62%. Similarly, Ottawa experienced an NPC increase of approximately 33% between the two sizing approaches. By comparison, lower NPC differences were observed in Abuja, Amman, Santiago, and Canberra, reflecting their comparatively lower variability and oversizing requirements. These results confirm that the economic penalty associated with reliability-oriented sizing becomes increasingly important as irradiance variability increases.

The substantial NPC increase observed in Paris and Ottawa agrees with previous findings that lifecycle costs are strongly influenced by climatic variability and reliability requirements. Yang et al. [83] showed that regions with less favorable renewable-energy resources require larger installed capacities to achieve acceptable supply reliability, thereby increasing overall system cost.

The LCOE comparison presented in Figure 16 reveals a more complex relationship between system cost and energy production. Although the average-based design generally exhibits the lowest CAPEX and NPC, it does not always produce the lowest LCOE. This occurs because LCOE depends on both lifecycle cost and the amount of useful energy delivered over the project lifetime. In Abuja and Amman, the average-based design produced slightly higher LCOE values than the daily-based and critical-month approaches despite its lower cost. Similarly, in Canberra and Santiago, the daily-based and critical-month designs achieved comparable or lower LCOE values than the average-based design. The highest LCOE values were observed in the critical-month designs for Paris (0.191 USD/kWh) and Ottawa (0.171 USD/kWh), indicating that the substantial increase in system size required to ensure reliability under highly variable climatic conditions is not fully offset by the corresponding increase in energy supply.

The non-linear relationship observed between NPC and LCOE is also consistent with previous techno-economic studies of standalone PV systems. Although lower investment costs generally contribute to lower LCOE, the metric is simultaneously affected by lifetime energy production and system utilization. As noted by Cristea et al. [84], systems with lower installed capacities may exhibit higher LCOE values if reductions in energy delivery outweigh the savings in capital cost. Consequently, the least expensive design does not necessarily correspond to the lowest unit cost of electricity.

A comparison across locations further highlights the influence of climatic conditions on economic performance. Abuja exhibits the highest LCOE values (0.223–0.228 USD/kWh), primarily due to higher localized component costs, higher discount rates, and faster battery degradation. In contrast, Santiago and Canberra achieve the lowest LCOE values, ranging from approximately 0.129 to 0.140 USD/kWh, reflecting favorable combinations of solar resource availability, moderate system sizes, lower degradation rates, and relatively lower lifecycle costs. Paris and Ottawa, despite their lower discount rates, experience elevated NPC and LCOE values because of the larger PV capacities required to compensate for seasonal solar resource variability.

The relatively higher LCOE values obtained in Abuja and Amman are consistent with studies showing that financing conditions, discount rates, and component procurement costs can significantly influence the economic viability of renewable-energy projects. IRENA [61] and the International Energy Agency [58] have reported that developing economies often experience higher project costs due to financing constraints, import dependencies, and elevated investment risks. Conversely, regions with mature renewable-energy markets and lower financing costs generally achieve lower lifecycle electricity costs.

Overall, the techno-economic results demonstrate a clear trade-off between system reliability and economic performance. While critical-month sizing improves reliability and reduces the risk of unmet load, it requires larger PV capacities and consequently higher CAPEX, OPEX, NPC, and, in some cases, LCOE. Conversely, average-based sizing minimizes investment costs but

may compromise system adequacy in regions with significant irradiance variability. The daily-based sizing approach generally provides an intermediate solution, balancing reliability improvements with moderate economic penalties. These findings are consistent with the conclusions of several recent studies that emphasize the importance of jointly considering reliability and economic criteria during off-grid PV system design rather than relying solely on cost-minimization approaches [85-87]. Therefore, incorporating irradiance variability into the techno-economic design process provides a more robust basis for selecting PV–battery system configurations capable of achieving an appropriate balance between cost, reliability, and long-term performance.

### 3.11 Implications for PV–battery system design

The results of this study demonstrate that solar irradiance variability exerts a significant influence on the technical and economic performance of standalone PV–battery systems. While average solar resource indicators provide useful preliminary information, they do not adequately capture the seasonal and day-to-day fluctuations that govern system reliability and long-term economic viability. Consequently, system designs based solely on average irradiation values may underestimate the PV capacity required to maintain reliable energy supply, particularly in regions characterized by high seasonal variability.

The comparative analysis reveals that climatic variability is a primary driver of PV oversizing requirements. Locations exhibiting high variability indices, such as Paris and Ottawa, require substantially larger PV capacities under the critical-month design approach to ensure acceptable reliability levels during prolonged low-irradiance periods. In contrast, locations with relatively stable solar resources, such as Abuja and Amman, can achieve comparable reliability with significantly lower oversizing requirements. These findings highlight the importance of incorporating variability metrics such as the coefficient of variation (CV) and seasonal variability index (SVI) into PV system design methodologies rather than relying exclusively on annual average irradiation values.

The reliability assessment further demonstrates that the selection of a sizing methodology has a direct impact on system adequacy. Average-based designs generally result in lower capital costs but may experience increased unmet load, higher LPSP values, and reduced reliability in locations with pronounced seasonal fluctuations. Conversely, critical-month sizing substantially improves system reliability by reducing energy deficits and loss-of-power-supply events. However, this reliability improvement is achieved at the expense of increased PV capacity, higher energy wastage, and greater investment costs. Therefore, the choice of sizing approach should be guided by the desired balance between reliability and economic affordability.

The battery aging analysis indicates that climatic conditions influence not only PV system design but also long-term storage performance. Higher ambient temperatures accelerate battery degradation and reduce battery lifetime, as observed in Abuja and Amman, whereas cooler locations such as Paris, Ottawa, and Santiago exhibit lower annual capacity fade rates and longer battery service lives. These results suggest that battery replacement scheduling and lifecycle costs should be explicitly considered during system planning, particularly in warm climates where thermal stress may significantly affect storage longevity.

The techno-economic analysis further reveals that reliability-oriented designs are not always economically optimal. Although critical-month sizing provides the highest reliability, it also results in increased CAPEX, OPEX, and NPC due to larger PV capacities and associated infrastructure requirements. Average-based designs generally achieve the lowest lifecycle costs but may compromise energy security in highly variable climates. The daily-based sizing approach offers an intermediate solution, providing improved reliability relative to average-based sizing while avoiding the excessive oversizing associated with critical-month design. Consequently, the most appropriate design strategy depends on the specific priorities of the application, whether reliability, affordability, or a compromise between both objectives.

Overall, the findings emphasize that effective standalone PV–battery system design requires an integrated assessment of solar resource variability, reliability requirements, battery aging characteristics, and economic performance. The study demonstrates that climate-responsive design approaches can substantially improve decision-making and enable the development of more reliable, cost-effective, and sustainable standalone energy systems across diverse climatic regions. These insights are particularly relevant for system designers, rural electrification planners, and policymakers seeking to optimize off-grid renewable energy deployment under varying environmental and economic conditions.

## 4. Conclusions

This study investigated the impact of solar irradiance variability on the sizing, reliability, battery aging, and techno-economic performance of standalone PV–battery systems across six climatically diverse locations: Abuja (Nigeria), Amman (Jordan), Paris (France), Ottawa (Canada), Santiago (Chile), and Canberra (Australia). By integrating irradiance variability metrics, multiple PV sizing approaches, daily energy-balance simulation, battery degradation assessment, and techno-economic analysis, the study provides a comprehensive evaluation of climate-responsive PV–battery system design.

The results reveal substantial differences in solar resource availability and variability among the selected locations. Abuja, Amman, and Santiago exhibited the highest average daily irradiation levels (approximately 5.60, 5.73, and 5.66 kWh/m²/day, respectively) and relatively low variability (CV/SVI ≈ 0.22/0.45 for Abuja, 0.40/0.99 for Amman, and 0.44/1.16 for Santiago), whereas Paris, Ottawa, and Canberra recorded lower irradiation levels (approximately 3.25, 3.59, and 4.74 kWh/m²/day, respectively) and the highest seasonal variability (CV/SVI ≈ 0.70/1.50 for Paris, 0.62/1.41 for Ottawa, and 0.49/1.35 for Canberra). The coefficient of variation and seasonal variability index confirmed that high-latitude locations experience significantly larger seasonal fluctuations in solar resource availability, thereby increasing system design complexity.

The comparative sizing analysis demonstrated that reliance on annual average irradiation can significantly underestimate PV capacity requirements in highly variable climates. Critical-month sizing produced the largest PV capacities and oversizing requirements, particularly in Paris and Ottawa, where PV capacities increased by approximately 188% and 332%, respectively, relative to average-based designs in order to maintain reliability during low-irradiance periods. In contrast, Abuja and Amman required considerably lower oversizing margins of approximately 39% and 89%, respectively, owing to their more stable solar resources. These findings demonstrate that irradiance variability, rather than average solar resource alone, is a key determinant of standalone PV system sizing.

The performance assessment further showed that larger PV capacities improve system reliability by reducing unmet load and loss-of-power-supply probability (LPSP). Systems designed using the critical-month approach achieved the highest reliability levels, with reliability indices approaching unity and LPSP values below 0.02. However, these reliability improvements were accompanied by increased wasted energy fractions, highlighting the trade-off between reliability and energy-utilization efficiency. Average-based designs generally resulted in lower investment costs but exhibited higher unmet load and lower reliability in regions with pronounced seasonal variability.

The battery aging analysis revealed that climatic conditions significantly influence long-term storage performance. Annual battery capacity fade ranged from approximately 1.46%/yr in cooler locations such as Paris, Ottawa, and Santiago to 1.73%/yr in Abuja. Consequently, battery lifetime varied from approximately 12.8 years in Abuja to about 15.2 years in Paris, Ottawa, and Santiago. These results indicate that elevated operating temperatures can accelerate storage degradation and increase battery replacement requirements over the project lifetime.

The techno-economic evaluation demonstrated that system costs are strongly influenced by both climatic conditions and sizing methodology. Critical-month sizing consistently resulted in the highest CAPEX, OPEX, and NPC values because of increased PV capacity requirements. In high-variability locations such as Paris and Ottawa, NPC increased by more than 30–60% relative to average-based designs. Although average-based sizing generally minimized lifecycle costs, it did not always produce the lowest LCOE because lower system capacities can reduce the amount of useful energy delivered over the project lifetime. The daily-based sizing approach provided a practical compromise between reliability and economic performance, offering improved adequacy relative to average-based sizing without the excessive oversizing associated with critical-month design.

Overall, the findings demonstrate that effective standalone PV–battery system design requires the explicit consideration of solar irradiance variability, battery degradation, reliability requirements, and lifecycle economics. The study confirms that climate-responsive sizing approaches provide a more robust basis for system design than conventional methods based solely on average solar resource indicators. The results provide valuable guidance for engineers, project developers, and policymakers involved in the planning and deployment of off-grid renewable-energy systems across diverse climatic regions.

The present study employed a daily energy-balance simulation framework for the technical

analysis, and therefore did not explicitly capture intra-day irradiance fluctuations, battery cycling dynamics, or short-term load variability. In addition, battery aging was evaluated using equivalent capacity-fade and lifetime estimates derived from PVsyst rather than detailed electrochemical degradation models. Future studies should incorporate high-resolution hourly irradiance and load data, advanced battery degradation and cycle-life models, and optimization-based techno-economic frameworks. Further investigations involving additional climatic regions, hybrid renewable-energy configurations, and demand-side management strategies would provide a broader understanding of the interactions among solar variability, storage requirements, system reliability, and economic performance.

**Acknowledgments**

The authors gratefully acknowledge the use of the PVGIS TMY 5.3 meteorological database, which provided the solar irradiance and climatic data utilized in this study. The authors also appreciate the valuable contributions of the developers and researchers whose work on standalone photovoltaic system modeling and renewable energy analysis provided useful insights for this research.

The authors sincerely acknowledge the moral support and encouragement of Mrs. Loveth Ohajianya during the preparation of this manuscript.

**Nomenclature**

| | |
|---|---|
| $AF$ | Annual capacity fade (%/year) |
| $AF_d$ | Annual capacity fade expressed as a decimal fraction |
| $C_0$ | Initial battery capacity (kWh) |
| $CAPEX$ | Capital expenditure (USD) |
| $C_{bat}$ | Battery cost (USD) |
| $C_{Batt}$ | Required battery storage capacity (kWh) |
| $C_{cost,t}$ | total expenditure incurred in year t (USD) |
| $C_{EOL}$ | Battery capacity at end-of-life (kWh) |
| $C_{FOB}$ | Global benchmark free-on-board cost (USD) |
| $C_{inv}$ | Inverter cost USD |
| $C_{local}$ | localized component cost (USD) |
| $C_{other}$ | Other components including installation and logistics (USD) |
| $C_{PV}$ | PV array cost (USD) |
| $CRF$ | Capital recovery factor |
| $C_t$ | Remaining battery capacity after t years (kWh) |
| $CV$ | Coefficient of variation |
| $DoD_{max}$ | Maximum allowable depth of discharge |
| $D_{PV}$ | Annual PV module degradation rate |
| $E_0$ | Initial annual energy production (kWh/yr) |
| $E_{actual}$ | Real PV output (kWh) |
| $E_d$ | Daily load demand (kWh/day) |
| $E_{def,d}$ | Unmet load on day $d$(kWh/day) |
| $E_{ideal}$ | Theoretical PV output under standard conditions (kWh) |
| $E_{PV,d}$ | PV energy generated on day $d$(kWh/day) |
| $E_t$ | Annual PV energy production in year t (kWh/yr) |
| $E_{waste,a}$ | Total annual wasted energy (kWh/year) |
| $E_{waste,d}$ | Wasted energy on day $t$(kWh/day) |
| $G$ | Solar irradiance (W/m²) |
| $GHI$ | Global horizontal irradiation (kWh/m$^2$) |
| $H_{avg}$ | Annual average daily irradiation (kWh/m²/day) |
| $H_{eq,d}$ | Equivalent daily peak sun hour |
| $H_{max}$ | Maximum monthly average daily irradiation (kWh/m²/day) |
| $H_{min}$ | Minimum monthly average daily irradiation (kWh/m²/day) |
| $i$ | Discount rate (%) |
| $L$ | Battery lifetime (years) |
| $LCOE$ | Levelized cost of energy (USD/kWh) |
| $LPSP$ | Loss of power supply probability |
| $M_{loc}$ | Location-specific cost multiplier |
| $n$ | Project lifetime (years) |
| $N_{aut}$ | Number of days of autonomy |
| $NOCT$ | Nominal operating cell temperature (°C) |
| $NPC$ | Net present cost (USD) |
| $OPEX$ | Operating expenditure (USD) |
| $P_{PV,avg}$ | Average-based PV capacity (kWp) |
| $P_{PV,crit}$ | Critical-month PV capacity (kWp) |
| $P_{PV,daily}$ | Daily-based PV capacity (kWp) |
| $PR$ | Performance ratio |

| | |
|---|---|
| $PR_{avg}$ | Average performance ratio |
| $PR_{crit}$ | Critical-month performance ratio |
| $PR_d$ | Daily performance ratio |
| $R$ | Reliability index |
| $SOC$ | State of charge |
| $SVI$ | Seasonal variability index |
| $T_a$ | Ambient temperature (°C) |
| $T_c$ | PV cell temperature (°C) |
| $\beta$ | Temperature coefficient (/$^0$C) |
| $\eta_{batt}$ | Battery efficiency |
| $\eta_{ch}$ | Battery charging efficiency |
| $\eta_{dis}$ | Battery discharging efficiency |
| $\eta_{inv}$ | Inverter efficiency |
| $\eta_{other}$ | Miscellaneous system efficiency |
| $\eta_{temp}$ | Temperature-loss factor |
| $\eta_{wire}$ | Wiring efficiency |
| $\sigma$ | Standard deviation of monthly irradiation |

## References


[1] Mujeeb, A., Oladigbolu, J., Bakare, M. S., & Ibrahim, A. A. (2025). Pathways to Environmental Sustainability through Energy Efficiency: A Strategic Next Energy Vision for Sustainable Development by 2050. *Scientific African*, e03053. DOI: 10.1016/j.sciaf.2025.e03053

[2] Rehman, A. U., Sanjari, M. J., Elavarasan, R. M., & Jamal, T. (2026). Sustainability-aligned pathways for energy transition: A review of low-carbon energy network solutions. *Renewable and Sustainable Energy Reviews*, *226*, 116428. DOI: 10.1016/j.rser.2025.116428

[3] Ali, A. O., Elgohr, A. T., El-Mahdy, M. H., Zohir, H. M., Emam, A. Z., Mostafa, M. G., Al-Razgan, M., Kasem, H. M., & Elhadidy, M. S. (2025). Advancements in photovoltaic technology: A comprehensive review of recent advances and future prospects. *Energy Conversion and Management: X*, *26*, 100952. DOI: 10.1016/j.ecmx.2025.100952

[4] Peters, I. M. (2025). Strategic Global Deployment of Photovoltaic Technology: Balancing Economic Capacity and Decarbonization Potential. *Advances in Atmospheric Sciences*, *42*(2), 261–268. DOI: 10.1007/s00376-024-4176-9

[5] Kishore, T. S., Kumar, P. U., & Ippili, V. (2025). Review of global sustainable solar energy policies: Significance and impact. *Innovation and Green Development*, *4*(2), 100224. DOI: 10.1016/j.igd.2025.100224

[6] Unegbu, H. C. O., Yawas, D. S., Dan-asabe, B., Alabi, A. A., & Vedad, R. C. (2025). Assessing the environmental and economic benefits of integrating solar energy in Nigerian construction. *Discover Civil Engineering*, *2*(1), 114. DOI: 10.1007/s44290-025-00274-0

[7] Ukoba, K., Yoro, K. O., Eterigho-Ikelegbe, O., Ibegbulam, C., & Jen, T.-C. (2024). Adaptation of solar energy in the Global South: Prospects, challenges and opportunities. *Heliyon*, *10*(7). DOI: 10.1016/j.heliyon.2024.e28009

[8] Come Zebra, E. I., van der Windt, H. J., Nhumaio, G., & Faaij, A. P. C. (2021). A review of hybrid renewable energy systems in mini-grids for off-grid electrification in developing countries. *Renewable and Sustainable Energy Reviews*, *144*, 111036. DOI: 10.1016/j.rser.2021.111036

[9] Mellaku, M. T., Wassie, Y. T., Seljom, P., & Adaramola, M. S. (2025). Decentralized renewable energy technology alternatives to bridge manufacturing sector energy supply-demand gap in East Africa: A systematic review of potentials, challenges, and opportunities. *Renewable and Sustainable Energy Reviews*, *216*, 115708. DOI: 10.1016/j.rser.2025.115708

[10] Al-Ali, S., Olabi, A. G., & Mahmoud, M. (2025). A review of solar photovoltaic technologies: developments, challenges, and future perspectives. *Energy Conversion and Management: X*, *27*, 101057. DOI: 10.1016/j.ecmx.2025.101057

[11] Uzorka, A., Kibirige, D., Mustafa, M. M., & Ukagwu, J. K. (2025). Design and implementation of a photovoltaic system for health facilities in rural areas of Uganda. *Discover Applied Sciences*, *7*(3), 197. DOI: 10.1007/s42452-025-06640-y

[12] Nsengimana, C., Kai, L., Yuhao, C., & Li, L. (2022). Standalone photovoltaic and battery microgrid design for rural areas. *Energy Exploration & Exploitation*, *40*(6), 1617–1633. DOI: 10.1177/01445987221102196

[13] Sepúlveda-Oviedo, E. H. (2025). Impact of environmental factors on photovoltaic system performance degradation. *Energy Strategy Reviews*, *59*, 101682. DOI: 10.1016/j.esr.2025.101682

[14] Alzahrani, M., Shanks, K., & Mallick, T. K. (2021). Advances and limitations of increasing solar irradiance for concentrating photovoltaics thermal system. *Renewable and Sustainable Energy Reviews*, *138*, 110517. DOI: 10.1016/j.rser.2020.110517

[15] Usman, Z., Tah, J., Abanda, H., & Nche, C. (2020). A Critical Appraisal of PV-Systems'

Performance. *Buildings*, *10*(11), 192. DOI: 10.3390/buildings10110192

[16] Jalomo-Cuevas, J., Colmenero Fonseca, F., Cárcel-Carrasco, J., Pérez, S. S., & Gudiño-Ochoa, A. (2023). Impact of Solar Radiation on Luminaires and Energy Efficiency in Isolated Residential Photovoltaic Systems. *Buildings*, *13*(10), 2655. DOI: 10.3390/buildings13102655

[17] Shaik, F., Lingala, S. S., & Veeraboina, P. (2023). Effect of various parameters on the performance of solar PV power plant: a review and the experimental study. *Sustainable Energy Research*, *10*(1), 6. DOI: 10.1186/s40807-023-00076-x

[18] Abed, M., Reddy B, A., Jyothsna, T. R., & Mohammed, N. (2025). Optimal sizing and performance assessment of stand-alone PV systems using optimum hybrid sizing strategy. *Results in Engineering*, *25*, 103793. DOI: 10.1016/j.rineng.2024.103793

[19] Bamisile, O., Acen, C., Cai, D., Huang, Q., & Staffell, I. (2025). The environmental factors affecting solar photovoltaic output. *Renewable and Sustainable Energy Reviews*, *208*, 115073. DOI: 10.1016/j.rser.2024.115073

[20] AlFaraj, J., Popovici, E., & Leahy, P. (2024). Solar Irradiance Database Comparison for PV System Design: A Case Study. *Sustainability*, *16*(15), 6436. DOI: 10.3390/su16156436

[21] Tavares, A. M., Conceição, R., Lopes, F. M., & Silva, H. G. (2024). Effect of Solar Irradiation Inter-Annual Variability on PV and CSP Power Plants Production Capacity: Portugal Case-Study. *Energies*, *17*(21), 5490. DOI: 10.3390/en17215490

[22] Ghodusinejad, M. H., Rashvand, N., Salmanpour, F., Danehkar, S., & Yousefi, H. (2026). A systematic review of solar irradiance forecasting across time horizons using physical, satellite, and AI-based methods. *Solar Compass*, *17*, 100154. DOI: 10.1016/j.solcom.2025.100154

[23] Soneye, O. O., Ayoola, M. A., Ajao, I. A., & Jegede, O. O. (2019). Diurnal and seasonal variations of the incoming solar radiation flux at a tropical station, Ile-Ife, Nigeria. *Heliyon*, *5*(5). DOI: 10.1016/j.heliyon.2019.e01673

[24] Lawin, A. E., Niyongendako, M., & Manirakiza, C. (2019). Solar Irradiance and Temperature Variability and Projected Trends Analysis in Burundi. *Climate*, *7*(6), 83. DOI: 10.3390/cli7060083

[25] İşler, B., Şener, U., Tokgözlü, A., Aslan, Z., & Heise, R. (2025). Spatio-Temporal Variation in Solar Irradiance in the Mediterranean Region: A Deep Learning Approach. *Sustainability*, *17*(15), 6696. DOI: 10.3390/su17156696

[26] Fathi, M., Allahyari, S., Ahmadi, A., Zahedi, A., & Asiaei, S. (2025). Enhanced global solar irradiance and temperature forecasting for rooftop PV power generation prediction using multi-step LSTM and GRU based hybrid models. *Energy Conversion and Management: X*, *28*, 101351. DOI: 10.1016/j.ecmx.2025.101351

[27] Pattath Gopi, N., & Devendran, S. (2015). Autonomy considerations for a standalone photovoltaic system. *Sustainable Energy Technologies and Assessments*, *10*, 79–83. DOI: 10.1016/j.seta.2015.03.005

[28] McCormick, P. G., & Suehrcke, H. (2018). The effect of intermittent solar radiation on the performance of PV systems. *Solar Energy*, *171*, 667–674. DOI: 10.1016/j.solener.2018.06.043

[29] Haruna, T., Ikot, A. N., & Big-Alabo, A. (2024). A Review of Factors Affecting the Efficiency and Output of PV Systems Applied in the Tropical Climate of South-South Nigeria. *African Journal of Advances in Science and Technology Research*, *16*(1), 01–17. DOI: 10.62154/ajastr.2024.016.010328

[30] Lotfy, A., Anis, W. R., Newagy, F., & Mohamed, S. M. (2025). Comparative Designs for Standalone Critical Loads Between PV/Battery and PV/Hydrogen Systems. *Hydrogen*, *6*(3), 46. DOI: 10.3390/hydrogen6030046

[31] Chatzigeorgiou, N. G., Theocharides, S., Makrides, G., & Georghiou, G. E. (2024). A review on battery energy storage systems: Applications, developments, and research trends of hybrid installations in the end-user sector. *Journal of Energy Storage*, *86*, 111192. DOI: 10.1016/j.est.2024.111192

[32] Maghami, M. R., Pasupuleti, J., Mutambara, A. G. O., & Ekanayake, J. (2025). Mitigation Technique Using a Hybrid Energy Storage and Time-of-Use (TOU) Approach in Photovoltaic Grid Connection. *Technologies*, *13*(8), 339. DOI: 10.3390/technologies13080339

[33] Quiles, E., Roldán-Blay, C., Escrivá-Escrivá, G., & Roldán-Porta, C. (2020). Accurate Sizing of Residential Stand-Alone Photovoltaic Systems Considering System Reliability. *Sustainability*, *12*(3), 1274. DOI: 10.3390/su12031274

[34] Okonkwo, P. C., Nwokolo, S. C., Udo, S. O., Obiwulu, A. U., Onnoghen, U. N., Alarifi, S. S., Eldosouky, A. M., Ekwok, S. E., Andráš, P., & Akpan, A. E. (2025). Solar PV systems under weather extremes: Case studies, classification, vulnerability assessment, and adaptation pathways.

*Energy Reports*, *13*, 929–959. DOI: 10.1016/j.egyr.2024.12.067

[35] Nallainathan, S., Arefi, A., Lund, C., & Mehrizi-Sani, A. (2025). Microgrid Reliability Incorporating Uncertainty in Weather and Equipment Failure. *Energies*, *18*(8), 2077. DOI: 10.3390/en18082077

[36] Perez, M., Perez, R., Rábago, K. R., & Putnam, M. (2019). Overbuilding & curtailment: The cost-effective enablers of firm PV generation. *Solar Energy*, *180*, 412–422. DOI: 10.1016/j.solener.2018.12.074

[37] Afonso, D., Mesbahi, O., Bouich, A., & Tlemçani, M. (2025). Influence of Long-Term and Short-Term Solar Radiation and Temperature Exposure on the Material Properties and Performance of Photovoltaic Panels: A Comprehensive Review. *Energies*, *18*(19), 5072. DOI: 10.3390/en18195072

[38] Carbajosa, C., Marín-Coca, S., Gavira-Aladro, M., & Martínez-Cava, A. (2025). Optimizing energy production in PV systems: Comprehensive review of radiation models and key factors influencing power generation. *Renewable Energy*, *249*, 123085. DOI: 10.1016/j.renene.2025.123085

[39] Omoriare, J. U., Ogherohwo, E. P., & Zhimwang, J. T. (2025). Investigating the influence of solar irradiance variability on the output power of photovoltaic (PV) systems in Akure, Nigeria. *World Journal of Applied Science & Technology*, *16*(1), 18–22. DOI: 10.4314/wojast.v16i1.18

[40] Ebhota, W. S., & Tabakov, P. Y. (2023). Influence of photovoltaic cell technologies and elevated temperature on photovoltaic system performance. *Ain Shams Engineering Journal*, *14*(7), 101984. DOI: 10.1016/j.asej.2022.101984

[41] Hudișteanu, V.-S., Cherecheș, N.-C., Țurcanu, F.-E., Hudișteanu, I., & Romila, C. (2024). Impact of Temperature on the Efficiency of Monocrystalline and Polycrystalline Photovoltaic Panels: A Comprehensive Experimental Analysis for Sustainable Energy Solutions. *Sustainability*, *16*(23), 10566. DOI: 10.3390/su162310566

[42] Jonasson, E., & Temiz, I. (2026). Evaluating complementarity: A review of metrics and their implications for hybrid renewable energy systems. *Renewable and Sustainable Energy Reviews*, *226*, 116422. DOI: 10.1016/j.rser.2025.116422

[43] Hashemian, N., & Noorpoor, A. (2023). Thermo-eco-environmental Investigation of a Newly Developed Solar/wind Powered Multi-Generation Plant with Hydrogen and Ammonia Production Options. *Journal of Solar Energy Research*, *8*(4), 1728–1737. DOI: 10.22059/jser.2024.374028.1388

[44] Hashemian, N., & Noorpoor, A. (2019). Assessment and multi-criteria optimization of a solar and biomass-based multi-generation system: Thermodynamic, exergoeconomic and exergoenvironmental aspects. *Energy Conversion and Management*, *195*, 788–797. DOI: 10.1016/j.enconman.2019.05.039

[45] Al-Maqsoosi, A., Al-Budairi, H., Akgündoğdu, A., & Al Yodaoi, H. (2026). Optimising Photovoltaic Power Output Using Hybrid Deep Reinforcement Learning and Real-Time Environmental Adaptation. *Journal of Solar Energy Research*, *11*(2), 2923–2933. DOI: 10.22059/jser.2026.410130.1708

[46] Chiteka, K., & Enweremadu, C. (2026). Numerical Investigation of Time-Dependent Dust Shading Effects on Fixed and Tracking Solar Photovoltaic Arrays. *Journal of Solar Energy Research*, *11*(2), 2934–2952. DOI: 10.22059/jser.2026.410193.1709

[47] Asgharzadeh Karamshahlu, A., Bahman Jahromi, H., & Saidi, M. H. (2026). A Novel Fan-Based Cooling System for Photovoltaic Panels: Impact on Thermal Regulation and Electrical Efficiency. *Journal of Solar Energy Research*, *11*(1), 2767–2779. DOI: 10.22059/jser.2026.407563.1679

[48] Faridah, L., Asnawi, R., Jati, H., & Kn, N. (2026). Techno-Economic Assessment and Optimization of Grid-Connected Solar Powered Electric Vehicle Charging Stations in Urban Indonesia. *Journal of Solar Energy Research*, *11*(1), 2835–2850. DOI: 10.22059/jser.2026.401157.1623

[49] Arora, J. S. (2012). Chapter 20 - Additional Topics on Optimum Design. In *Introduction to Optimum Design (Third Edition)* (pp. 731–784). Academic Press. DOI: 10.1016/B978-0-12-381375-6.00029-2

[50] Abo-Khalil, A. G., Sayed, K., Radwan, A., & El-Sharkawy, I. A. (2023). Analysis of the PV system sizing and economic feasibility study in a grid-connected PV system. *Case Studies in Thermal Engineering*, *45*, 102903. DOI: 10.1016/j.csite.2023.102903

[51] Jivaganont, P., Limthongkul, P., & Mongkoltanatas, J. (2024). Design of photovoltaic and battery energy storage systems through load demand characterization: A case study in Thailand. *Energy Reports*, *12*, 4578–4593. DOI: 10.1016/j.egyr.2024.10.025

[52] Michael-Ahile, T., Samuels, J. A., & Booysen, M. J. (2025). Optimizing battery energy storage and solar photovoltaic systems for lower-to-middle-income schools amidst load-shedding. *Energy for*

*Sustainable Development*, *85*, 101675. DOI: 10.1016/j.esd.2025.101675
[53] Šimić, Z., Barukčić, M., Knežević, G., & Topić, D. (2025). Optimization of an Off-Grid PV System with Respect to the Loss of Load Probability Value. *Energies*, *18*(19), 5174. DOI: 10.3390/en18195174
[54] Shen, L., Li, Z., & Ma, T. (2020). Analysis of the power loss and quantification of the energy distribution in PV module. *Applied Energy*, *260*, 114333. DOI: 10.1016/j.apenergy.2019.114333
[55] Jacob, A. S., Banerjee, R., & Ghosh, P. C. (2020). Trade-off between end of life of battery and reliability in a photovoltaic system. *Journal of Energy Storage*, *30*, 101565. DOI: 10.1016/j.est.2020.101565
[56] Fischer, M., Brand, M. J., Karger, A., Gomez, M. R., Rehm, M., Natterer, J., & Jossen, A. (2025). How degradation of lithium-ion batteries impacts capacity fade and resistance increase: A systematic, correlative analysis. *Journal of Power Sources*, *656*, 237921. DOI: 10.1016/j.jpowsour.2025.237921
[57] Nagde, K. R., & Dhoble, S. J. (2021). Chapter 12 - Li-S ion batteries: a substitute for Li-ion storage batteries. In S. J. Dhoble, N. T. Kalyani, B. Vengadaesvaran, & A. Kariem Arof (Eds.), *Energy Materials* (pp. 335–371). Elsevier. DOI: 10.1016/B978-0-12-823710-6.00008-X
[58] IEA-PVPS. (2025). *Trends in Photovoltaic Applications 2025*. International Energy Agency Photovoltaic Power Systems Programme Retrieved from https://iea-pvps.org/wp-content/uploads/2025/10/IEA-PVPS_Trends_2025-.pdf
[59] BloombergNEF. (2025). *2025 Lithium-Ion Battery Price Survey*. Bloomberg New Energy Finance, London, Technical Report Retrieved from https://www.evinfrastructurenews.com/ev-technology/bloomberg-nef-lithium-ion-battery-pack-prices-drop-worldwide-ev-applications-hit-by-higher-materials-cost
[60] NREL. (2026). *Annual Technology Baseline: Solar Photovoltaic and Energy Storage Cost Benchmarks*. U.S. Department of Energy, Golden, CO, Technical Report Retrieved from https://www.nlr.gov/solar/market-research-analysis/solar-installed-system-cost
[61] IRENA. (2025). *Renewable Power Generation Costs*. International Renewable Energy Agency, Abu Dhabi, Technical Report Retrieved from https://www.irena.org/-/media/Files/IRENA/Agency/Publication/2025/Jul/IRENA_TEC_RPGC_in_2024_2025.pdf
[62] Ohajianya, A. C., Ezihe, J. A., Nwaneho, F. U., Ouserigha, E. C., Echewodo, J. C., & Ugbaja, C. M. (2026). Techno-economic comparison of lead-acid and lithium-ion batteries in residential PV systems: A multi-location study of Abuja, Beijing, and Washington DC. *Journal of Asian Energy Studies*, *10*, 17–38. DOI: 10.24112/jaes.100003
[63] Talavera, D. L., Muñoz-Cerón, E., de la Casa, J., Lozano-Arjona, D., Theristis, M., & Pérez-Higueras, P. J. (2019). Complete Procedure for the Economic, Financial and Cost-Competitiveness of Photovoltaic Systems with Self-Consumption. *Energies*, *12*(3), 345. DOI: 10.3390/en12030345
[64] Gong, D., Xu, J., & Yan, J. (2023). National development banks and loan contract terms: Evidence from syndicated loans. *Journal of International Money and Finance*, *130*, 102763. DOI: 10.1016/j.jimonfin.2022.102763
[65] Agyekum, E. B., Odoi-Yorke, F., Abbey, A. A., Adegboye, O. R., & Rashid, F. L. (2025). Techno-economic, social and environmental analysis of different photovoltaic cell technologies under tropical weather conditions. *International Journal of Thermofluids*, *27*, 101164. DOI: 10.1016/j.ijft.2025.101164
[66] Ijeoma, M. W., Chen, H., Carbajales-Dale, M., & Yakubu, R. O. (2023). Techno-Economic Assessment of the Viability of Commercial Solar PV System in Port Harcourt, Rivers State, Nigeria. *Energies*, *16*(19), 6803. DOI: 10.3390/en16196803
[67] Chauhan, A., & Saini, R. P. (2016). Techno-economic feasibility study on Integrated Renewable Energy System for an isolated community of India. *Renewable and Sustainable Energy Reviews*, *59*, 388–405. DOI: 10.1016/j.rser.2015.12.290
[68] Gomes, J., Cabral, D., & Karlsson, B. (2022). Defining an Annual Energy Output Ratio between Solar Thermal Collectors and Photovoltaic Modules. *Energies*, *15*(15), 5577. DOI: 10.3390/en15155577
[69] Ogunjuyigbe, A. S. O., Ayodele, T. R., & Alao, M. A. (2017). Electricity generation from municipal solid waste in some selected cities of Nigeria: An assessment of feasibility, potential and technologies. *Renewable and Sustainable Energy Reviews*, *80*, 149–162. DOI: 10.1016/j.rser.2017.05.177
[70] Berna-Escriche, C., Álvarez-Piñeiro, L., & Blanco, D. (2025). Forecasts Plus Assessments of Renewable Generation Performance, the Effect of Earth's Geographic Location on Solar and Wind Generation. *Applied Sciences*, *15*(3), 1450. DOI: 10.3390/app15031450
[71] Okoye, C. O., Taylan, O., & Baker, D. K. (2016). Solar energy potentials in strategically located cities in Nigeria: Review, resource assessment and PV system design. *Renewable and*

*Sustainable Energy Reviews*, *55*, 550–566. DOI: 10.1016/j.rser.2015.10.154

[72] Scipioni, R., Marocco, P., Juel, M., Kauko, H., Sundseth, K., & Santarelli, M. (2026). Building Resilient Off-Grid Energy Systems: Hybrid Storage Solutions for Cold Climates. In R. Scipioni, M. E. Gil Bardají, L. Barelli, M. Baumann, & S. Passerini (Eds.), *Hybrid Energy Storage: Case Studies for the Energy Transition* (pp. 143–181). Springer Nature Switzerland. DOI: 10.1007/978-3-031-97755-8_7

[73] Sanchís-Gómez, C., Aleix-Moreno, J., Vargas-Salgado, C., & Alfonso-Solar, D. (2025). Towards More Sustainable Photovoltaic Systems: Enhanced Open-Circuit Voltage Prediction with a New Extreme Meteorological Year Model. *Sustainability*, *17*(16), 7554. DOI: 10.3390/su17167554

[74] Đurin, B., & Plantak, L. (2018). 'Worst Month' and 'Critical Period' Methods for the Sizing of Solar Irrigation Systems – A Comparison. *Revista Facultad De Ingeniería Universidad De Antioquia*(88), 100–109. DOI: 10.17533/udea.redin.n88a11

[75] Kahsay, M. B., & Lauwaert, J. (2022). Excess Energy from PV-Battery System Installations: A Case of Rural Health Center in Tigray, Ethiopia. *Energies*, *15*(12), 4355. DOI: 10.3390/en15124355

[76] Nadeem, T. B., Siddiqui, M., Khalid, M., & Asif, M. (2023). Distributed energy systems: A review of classification, technologies, applications, and policies. *Energy Strategy Reviews*, *48*, 101096. DOI: 10.1016/j.esr.2023.101096

[77] Rumbayan, M., Kindangen, J., Sambul, A., Sompie, S., & Cross, J. (2025). Solar energy implementation in rural communities and its contributions to SDGs: A systematic literature review. *Unconventional Resources*, *6*, 100180. DOI: 10.1016/j.uncres.2025.100180

[78] Tor, T., Nyam, G. G., Samson, D. O., Asake, J., & Iortim, D. M. (2025). Assessment of Solar Energy Potential and Radiation Impact in the Federal Capital Territory and Nasarawa State, Nigeria. *Faculty of Natural and Applied Sciences Journal of Applied and Physical Sciences*, *2*(3), 54–65. DOI: 10.63561/japs.v2i3.814

[79] Liu, H., Wu, B., Maleki, A., Pourfayaz, F., & Ghasempour, R. (2021). Effects of Reliability Index on Optimal Configuration of Hybrid Solar/Battery Energy System by Optimization Approach: A Case Study. *International Journal of Photoenergy*, *2021*(1), 9779996. DOI: 10.1155/2021/9779996

[80] Asiri, M., Kedhim, M., Jain, V., Ballal, S., Singh, A., Kavitha, V., Kamolova, N., & Nourizadeh, M. (2025). Impact of temperature and state-of-charge on long-term storage degradation in lithium-ion batteries: an integrated P2D-based degradation analysis. *RSC Advances*, *15*(28), 22576–22586. DOI: 10.1039/d5ra03735b

[81] Belmahdi, B., & Bouardi, A. E. (2020). Solar Potential Assessment using PVsyst Software in the Northern Zone of Morocco. *Procedia Manufacturing*, *46*, 738–745. DOI: 10.1016/j.promfg.2020.03.104

[82] Lee, J. T., & Callaway, D. S. (2018). The cost of reliability in decentralized solar power systems in sub-Saharan Africa. *Nature Energy*, *3*(11), 960–968. DOI: 10.1038/s41560-018-0240-y

[83] Yang, Y., Wei, Q., Liu, S., & Zhao, L. (2022). Distribution Strategy Optimization of Standalone Hybrid WT/PV System Based on Different Solar and Wind Resources for Rural Applications. *Energies*, *15*(14), 5307. DOI: 10.3390/en15145307

[84] Cristea, M., Cristea, C., Tîrnovan, R.-A., & Șerban, F. M. (2025). Levelized Cost of Energy (LCOE) of Different Photovoltaic Technologies. *Applied Sciences*, *15*(12), 6710. DOI: 10.3390/app15126710

[85] Nyarko, K., Whale, J., & Urmee, T. (2023). Drivers and challenges of off-grid renewable energy-based projects in West Africa: A review. *Heliyon*, *9*(6), e16710. DOI: 10.1016/j.heliyon.2023.e16710

[86] Akinsipe, O. C., Moya, D., & Kaparaju, P. (2021). Design and economic analysis of off-grid solar PV system in Jos-Nigeria. *Journal of Cleaner Production*, *287*, 125055. DOI: 10.1016/j.jclepro.2020.125055

[87] Liao, R., Manfren, M., & Nastasi, B. (2025). Off-grid PV systems modelling and optimisation for rural communities - leveraging understandability and interpretability of modelling tools. *Energy*, *324*, 135948. DOI: 10.1016/j.energy.2025.135948